# Reactions of 1-Hydroxy-1-methylethyl Radicals with NO 2 - : Time-Resolved Electron Spin Resonance

**ARTICLE** *in* THE JOURNAL OF PHYSICAL CHEMISTRY A · OCTOBER 2006

Impact Factor: 2.69 · DOI: 10.1021/jp062398c · Source: PubMed



**5 AUTHORS**, INCLUDING:

Piotr Filipiak
Adam Mickiewicz University
**18** PUBLICATIONS **167** CITATIONS
SEE PROFILE

Lily Hug
University of Greenwich
**114** PUBLICATIONS **2,664** CITATIONS
SEE PROFILE

# Reactions of 1-Hydroxy-1-methylethyl Radicals with $NO_2^-$: Time-Resolved Electron Spin Resonance

**Piotr Filipiak,[†] Donald M. Camaioni,[‡] Richard W. Fessenden,[†] Ian Carmichael,[†] and Gordon L. Hug*[,†,§,#]**

*Radiation Laboratory, University of Notre Dame, Notre Dame, Indiana 46556, Pacific Northwest National Laboratory, P.O. Box 999, Richland, Washington 99352, and Faculty of Chemistry, Adam Mickiewicz University, 60-780 Poznan, Poland*

*Received: April 19, 2006; In Final Form: July 26, 2006*

The reaction of the α-hydroxyalkyl radical of 2-propanol (1-hydroxy-1-methylethyl radical) with nitrite ions was characterized. A product of the reaction was assigned as the adduct nitro radical anion, $[HO-C(CH_3)_2NO_2]^{\bullet-}$. This radical was identified using time-resolved electron spin resonance (TRESR). The radical's magnetic parameters, the nitrogen hyperfine coupling constant ($a_N$ = 26.39 G), and its *g*-factor (2.0052) were the same as those of the nitro radical anion previously discovered in $^{\bullet}OH$ spin-trapping experiments with the *aci*-anion of $(CH_3)_2CHNO_2$. Production of $[HO-C(CH_3)_2NO_2]^{\bullet-}$ was determined to be 38% ± 4% of the reaction of $(CH_3)_2C^{\bullet}-OH$ with nitrite. The reason why this fraction was less than 100% was rationalized by invoking the competitive addition at oxygen, which forms $[HO-C(CH_3)_2ONO]^{\bullet-}$, followed by a rapid loss of $^{\bullet}NO$. Furthermore, by taking this mechanism into account, the bimolecular rate constant for the total reaction of $(CH_3)_2C^{\bullet}-OH$ with nitrite at reaction pH 7 was determined to be $1.6 \times 10^6$ $M^{-1}$ $s^{-1}$, using both decay traces of $(CH_3)_2C^{\bullet}-OH$ and growth traces of $[HO-C(CH_3)_2NO_2]^{\bullet-}$. This correspondence further confirms the nature of the reaction. The reaction mechanism is discussed with guidance by computations using density functional theory.

## Introduction

The nature of the reaction of organic radicals with nitrite ions is not as straightforward as it might appear at first glance. Recently, there was a controversy in regard to whether an H atom (a prototype for organic radicals) adds to an O atom[1] or to the N atom[2] of a nitrite anion. Because nitrite is a redox agent, its reactions with redox active organic radicals have the added complication that electron-transfer pathways could also be involved.

As a practical matter, the reaction of reducing radicals with nitrite has become important in assessing the fate of organic complexants in nuclear waste that is stored in tanks at Hanford and Savannah river sites.[3] Typically, the aqueous wastes contain ∼1 M nitrite and several molar nitrate ions, along with glycolate and aminopolycarboxylates that have been added to complex the radioactive metal ions. These complexants are susceptible to radiolytic fragmentations, leading to reducing radicals such as hydroxymethyl and α-aminoalkyl radicals. After the organic radicals are formed, their most likely reaction partners are the $NO_x$ ions, because of the high concentrations of the latter species. Aging of organic complexants in the wastes is a safety concern, because of the potential formation of flammable mixtures of gases in the tanks.[4]

An early report on photoinduced reactions of nitrite and alcohols in basic aqueous solution invoked a reaction of the alcohol radicals with nitrite to explain the appearance of nitro radical anions detected by electron spin resonance (ESR).[5] In these steady-state irradiations, the nitrite ions were presumably photodissociated to $^{\bullet}NO$ and $O^{\bullet-}$, and then $O^{\bullet-}/^{\bullet}OH$ abstracted H atoms from the alcohols.[6−9] The resulting alcohol radicals then reacted with unreacted nitrite to form the nitro radical anion via a free-radical mechanism that was suggested by Kornblum.[10] The mechanism of the reaction of alcohol radical with nitrite was not discussed in any further detail.[5]

The same adduct was also postulated to be an intermediate in the overall reduction of nitrite ions to $^{\bullet}NO$ by 1-hydroxy-1-methylethyl radicals in steady-state radiolysis of aqueous solutions of nitrite, 2-propanol, and acetone.[11] No direct observation of the adduct was made. The suggested[11] intermediate was based on the analogy to an adduct radical formed between $EtO-^{\bullet}CHMe$ and nitrite.[12] The latter work contained an ESR observation of the adduct radical, where $EtO-^{\bullet}CHMe$ was produced in a $Ti^{III}-H_2O_2$ system, which oxidized diethyl ether.

To assess further the mechanism of the reaction of reducing organic radicals with nitrite ions, we have examined the reaction of the 1-hydroxy-1-methylethyl radical with nitrite. Instead of using photochemical excitation, we have used controlled radiolytic situations, wherein the alcohol radical was predominantly formed, and both the precursor and successor radicals were monitored by time-resolved electron spin resonance (TRESR). Insight into alternate reaction pathways was gained through computations using density functional theory (DFT). DFT calculations were also used to evaluate the magnetic properties of the various radicals observed in this work.

* Author to whom correspondence should be addressed. Tel.: 574-631-4504, -6163, -7441. Fax: 574-631-8068. E-mail address: hug.1@nd.edu.
† Radiation Laboratory, University of Notre Dame.
‡ Pacific Northwest National Laboratory.
§ Faculty of Chemistry, Adam Mickiewicz University.
# Fulbright Scholar, Faculty of Chemistry, Adam Mickiewicz University. Permanent address: Radiation Laboratory, University of Notre Dame.

10.1021/jp062398c CCC: $33.50 
Published on Web 08/31/2006

## Experimental Section

**Materials.** Acetone was high-performance liquid chromatography (HPLC) grade, from Fisher Scientific; the 2-propanol used was also from Fisher Scientific. Sodium nitrite was obtained from J.T. Baker Chemical Co., and 2-nitropropane was purchased from Aldrich Chemical Co. Buffered solutions at neutral pH used 1 mM buffers of equal molar amounts of sodium phosphate monobasic and sodium phosphate dibasic salts from Fisher Scientific. The deionized water, which was used in making the solutions, was purified in a reverse osmosis/deionization system from a Serv-A-Pure Co. There is an UV-irradiation unit in the circulating section of this water-purification system. The purity of the water exceeded that of triply distilled water. Typically, this water has a resistance of >18 MΩ cm and a total organic carbon (TOC) content of <10 ppb.

**Time-Resolved Electron Spin Resonance (TRESR).** Free radicals were produced from the pulse radiolysis of aqueous solutions. The source of radiation was 2.8 MeV electrons from a Van de Graaff accelerator operated in the pulsed mode (pulse width of 0.5 $\mu$s). The resulting radicals were detected via ESR. The ESR spectrometer and its operation, in conjunction with the Van de Graaff accelerator, have been described elsewhere.[13−15] The X-band microwaves (9.35 GHz) for the ESR detection were not pulsed; however, there is direct detection (no field modulation) of the ESR signal, which allows for the accumulation of data in time-resolved modes, analogous to optical detection of transients in pulse radiolysis and laser flash photolysis. In this work, the ESR spectrometer was used both in the kinetic mode, when kinetic traces were needed to determine rate constants, and in the "boxcar" mode, to obtain spectra of the radicals in fixed time windows following the radiolysis pulse. For spectral positions of the ESR lines, the magnetic fields are quoted in gauss (G), but as a displacement from the magnetic field, corresponding to $g = 2.00043$. This is the zero of the $\Delta B_0$ scale quoted in this paper.

The sample solutions were flowed at rates of 10−15 cm$^3$/min through a quartz cell 0.4 mm thick. The solutions were cooled and run through a bubble trap[16] before entering the quartz cell in the resonant microwave cavity. The temperature of the solution upon exiting the ESR cell was 13 °C. The cell was oriented within the microwave resonant cavity $(TE)_{102}$, such that accelerated electrons were incident edge-on to the cell and such that the microwave magnetic field was maximum in the plane of the cell's broad face. Further details on the current configuration of the ESR spectrometer and Van de Graaff accelerator can be found in other recent work.[17]

**Yields from TRESR.** A methodology was recently developed to measure radical yields from kinetic traces formed from the direct detection of TRESR.[18] In ESR, the number of radicals (or concentration of radicals in a fixed volume) is related to the total area of the ESR lines of a spectrum. In the mentioned work,[18] the amplitudes of the kinetic traces of selected lines were measured and the widths taken into account by modeling the width by means of the spin relaxation times ($T_1$ and $T_2$) and the line broadening by the magnetic field inhomogeneity ($W$). Simply stated, the yields are determined by comparing the relative "intensity" of the radical under study and that of the sulfite radical via kinetic traces taken at the centers of selected ESR spectral lines of the two radicals. Thus, for the intensities (or scale factors) of the kinetic traces to represent the true area under an ESR line, the various spin relaxation times ($T_1$ and $T_2$), the chemical rates, and relevant instrumental factors must be measured and factored into the computation of a predicted ESR time profile. The kinetic traces were simulated by numerical integration of modified Bloch equations,[13] the "modification" of which takes into account the chemical reaction mechanism and kinetics and any chemical-induced dynamic electron polarization (CIDEP). Initially, the Bloch equations are scaled (arbitrarily) so that the Boltzmann value of the $z$-axis magnetization is equal to the micromolar radical concentration. An additional scale factor is needed to match the calculated ESR amplitude to the experimental data for the respective kinetic traces (taking into account instrumental factors). Each radical at a given concentration will have the same basic scale factor. The value for a particular ESR line then takes into account the degeneracy represented by the number and statistical intensity of the hyperfine lines. Thus, if the concentration is properly represented by the kinetic mechanism, the actual scale factor needed to fit the observed ESR amplitude will be that predicted from that of the reference radical. The scale factor will vary from day to day, because the position of the cell in the cavity affects the $Q$-factor. However, the value for $^{\bullet}SO_3^-$ has been determined to be constant at 10, within approximately ±20%, over many years.

**TABLE 1: Parameters Used in Modeling ESR Responses**

| radical | $T_1$ | $T_2$ |
|---|---|---|
| $^{\bullet}SO_3^-$ | 1.6 $\mu$s | 1.6 $\mu$s |
| $^-O_2CCH{=}C^{\bullet}CO_2^-$ | 7.1 $\mu$s | 6.1 $\mu$s |
| $(CH_3)_2C^{\bullet}-OH$ | 1.3 $\mu$s | 1.3 $\mu$s |
| $[HO-C(CH_3)_2NO_2]^{\bullet-}$ | 0.38 $\mu$s | 0.38 $\mu$s |
| inhomogeneity parameter, $W$[a] | 20 mG | |
| microwave magnetic field, $B_1$ | 16 mG at −10 dB | |

[a] Full width at half-height of a Gaussian distribution.

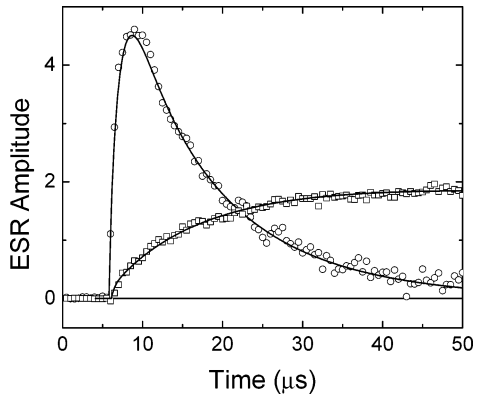


**Figure 1.** Kinetic traces of the central lines of the precursor and successor radicals. A $N_2$-saturated aqueous solution of 0.1 M 2-propanol, 0.4 M acetone, and 25 mM sodium nitrite with 1 mM phosphate buffer (pH 7) was used. The open circles show the kinetic trace of the $(CH_3)_2C^{\bullet}-OH$ radical at $\Delta B_0 = -4.77$ G, and the square points show the kinetic trace of the $[HO-C-(CH_3)_2NO_2]^{\bullet-}$ radical at $\Delta B_0 = -8.10$ G. Solid lines represent simulations as described later in this work. The vertical scale is given in arbitrary units, but the relative amplitudes of the two curves are as observed.

The parameters that must be determined for proper modeling of the ESR responses are given in Table 1. The iterative methodology for determining these parameters is described in more detail in the Supporting Information. The fit to the decay of $(CH_3)_2C^{\bullet}-OH$ and the growth of the adduct in a particular experiment is shown in Figure 1. Because all the physical and chemical parameters were incorporated into these simulations, there is only a single scale factor left for each kinetic trace. These scale factors give the relative yield of the adduct, with respect to that of the reference radical, $^{\bullet}SO_3^-$, after one takes

into account the degeneracy of the monitored ESR line of the adduct radical.

The radiation-chemical yield ($G$, in ionizations per 100 eV of radiation absorbed) for $(CH_3)_2C^{\bullet}-OH$ in the absence of nitrite was taken to be the sum of the $G$'s for $e_{aq}^-$, $^{\bullet}OH$, and $H^{\bullet}$. It is recognized that all of the reaction of $^{\bullet}OH$ with 2-propanol does not form $(CH_3)_2C^{\bullet}-OH$ and that the relatively high concentrations of 2-propanol and acetone used to form $(CH_3)_2C^{\bullet}-OH$ may raise the yields ($G$'s) from the lower concentration values somewhat. The main place where the yield ($G$) matters is in the comparison of the ESR intensity of $(CH_3)_2C^{\bullet}-OH$ and $^{\bullet}SO_3^-$. The calculations assumed that the radiation−chemical yield of $^{\bullet}SO_3^-$ (in $N_2O$-saturated solution) was equal to the sum of those for $e_{aq}^-$ and $^{\bullet}OH$. The inclusion of the radiation−chemical yield for $H^{\bullet}$, in the case of 2-propanol, was assumed to compensate for the portion of the $^{\bullet}OH$ reaction that does not give $(CH_3)_2C^{\bullet}-OH$.

**Computational Details.** Density functional theory (DFT) calculations were performed with local versions of the Gaussian98[19] and Dalton[20] electronic structure software packages that apply the B3LYP functional.[21] This hybrid functional comprises both local[22] and nonlocal (gradient-corrected) exchange[23] and correlation[24,25] contributions, mixed with a piece of exact (Hartree−Fock) exchange. The mixing parameters are derived from fits to known thermochemistry of a well-characterized set of small molecules. For structural studies, a polarized split-valence basis set, augmented with heavy atom diffuse *s*- and *p*-functions, was used (denoted 6-31+G*). DFT geometries are often converged with modest basis sets. EPR parameters were obtained using a basis set specifically designed to recover accurate Fermi contact interactions.[26] The *g*-factors were obtained as shifts from the free-electron value by a coupled-perturbed self-consistent field scheme given by Neese.[27] Solvent effects were recovered by reoptimizing the geometrical structures in a self-consistent isodensity reaction field,[28] using an isodensity contour of 0.001 au and then recomputing the magnetic properties in the presence of a COSMO[29] reaction field parametrized for water.[30]

## Results and Discussion

The radiolysis of water,

$$H_2O \rightsquigarrow e_{aq}^-, {}^{\bullet}OH, H^{\bullet}, H^+ \quad (1)$$

is a convenient way to produce strongly reducing radicals (hydrated electrons and H atoms) and oxidizing radicals (hydroxyl radical) that can be scavenged by appropriate substrates to generate radicals of interest. It is possible to take advantage of all these primary radicals to generate $(CH_3)_2C^{\bullet}-OH$ by choosing a mixture of substrates, 2-propanol and acetone,

$$(CH_3)_2CH-OH + {}^{\bullet}OH \rightarrow (CH_3)_2C^{\bullet}-OH + H_2O \quad (2)$$

with a rate constant of $1.9 \times 10^9$ $M^{-1}$ $s^{-1}$,[31]

$$(CH_3)_2C{=}O + e_{aq}^{\bullet} \rightarrow (CH_3)_2C^{\bullet}-O^- \quad (3)$$

with a rate constant of $6.5 \times 10^9$ $M^{-1}$ $s^{-1}$,[31] to form radical anions (which protonate to form the desired radicals), and

$$(CH_3)_2CH-OH + H^{\bullet} \rightarrow (CH_3)_2C^{\bullet}-OH + H_2 \quad (4)$$

with a rate constant of $9.0 \times 10^7$ $M^{-1}$ $s^{-1}$.[32] The reaction that we wanted to isolate and study was the reaction of $(CH_3)_2C^{\bullet}-OH$ with nitrite ions. Nitrite ions also react rapidly with all the primary radicals: $6.0 \times 10^9$ $M^{-1}$ $s^{-1}$ with $^{\bullet}OH$,[33] $3.5 \times 10^9$ $M^{-1}$ $s^{-1}$ with $e_{aq}^-$,[33] and $1.6 \times 10^9$ $M^{-1}$ $s^{-1}$ with $H^{\bullet}$.[1]

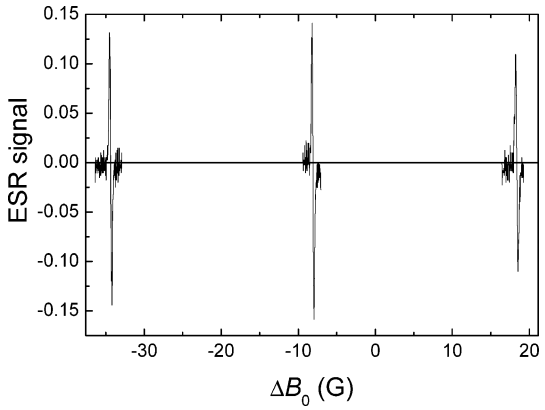


**Figure 2.** Time-resolved spectrum taken in the time window of 60−75 $\mu$s, following the 0.5 $\mu$s radiolytic pulse. A $N_2$-saturated aqueous solution of 0.1 M 2-propanol, 0.1 M acetone, and 10 mM sodium nitrite with a 1 mM phosphate buffer (pH 7) was used. The zero for the scale of magnetic field offset ($\Delta B_0$) is taken as the resonance condition for the radicals in quartz, corresponding to a line at $g = 2.00043$.

$$NO_2^- + {}^{\bullet}OH \rightarrow {}^{\bullet}NO_2 + OH^- \quad (5)$$

$$NO_2^- + e_{aq}^- \rightarrow {}^{\bullet}NO_2^{2-} + (H_2O) \rightarrow {}^{\bullet}NO + 2OH^- \quad (6)$$

$${}^{\bullet}NO_2^{2-} + H_2O \rightarrow {}^{\bullet}NO + 2OH^- \quad (7)$$

$$NO_2^- + H^{\bullet} \rightarrow H-{}^{\bullet}NO_2^- \quad (8)$$

$$H-{}^{\bullet}NO_2^- + HB \rightarrow {}^{\bullet}NO + H_2O + B^- \quad (9)$$

In the presence of a buffer, HB, $H-{}^{\bullet}NO_2^-$ converts to $^{\bullet}NO$, and the rate constant for $H_2PO_4^-$ is such that this will occur within a few microseconds.[2]

To reduce complications with radicals formed from these reactions of nitrite ions with the primary radicals that come from the radiolysis of water, the concentrations of 2-propanol and acetone were normally set at 0.1 M (and higher), and the concentrations of nitrite was normally ≤25 mM. In considering the radiation chemical yields, however, it will be necessary to take into account these competitive reactions for the primary radicals. Other concentration conditions were used to test various points of interest.

**Assignment of the Radical (Spectrum and Kinetics).** When a nitrogen-saturated aqueous solution containing 0.1 M of both 2-propanol and acetone and 10 mM of nitrite was irradiated, three ESR lines appeared that were not associated with $(CH_3)_2C^{\bullet}-OH$. These three lines are shown in Figure 2. The lines are of almost equal intensity, which suggests a nitrogen splitting. If so, the hyperfine splitting, $a_N$, is 26.39 G, taking into account second-order shifts,[34] and the *g*-factor is 2.0052.

One nitrogen radical that would seem a likely candidate for this radical is $^{\bullet}NO_2^{2-}$, because α-hydroxyalkyl radicals are strongly reducing radicals. In particular, the redox couple relevant for electron-transfer reaction 10 is $E^0[(CH_3)_2C{=}O, H^+/(CH_3)_2C^{\bullet}-OH] = -1.39$ V vs NHE.[35]

$$(CH_3)_2C^{\bullet}-OH + NO_2^- \rightarrow {}^{\bullet}NO_2^{2-} + (CH_3)_2CO + H^+ \quad (10)$$

However, this reaction will be followed quickly by reaction 7, where the rate constant for decay of $^{\bullet}NO_2^{2-}$ is $1.6 \times 10^6$ $s^{-1}$, so the lifetime should be <1 $\mu$s.[2]

In addition, the spectrum in Figure 2 is distinctly different than what might be expected for $^{\bullet}NO_2^{2-}$; various anisotropic spectra in solids attributed to this radical have been analyzed with an isotropic nitrogen hyperfine splitting of $a_N = 9.5-16$ G and an isotropic *g*-factor of 2.0026−2.005.[36−42] For $^{\bullet}NO_2^{2-}$, the DFT calculations described previously give a *g*-factor of 2.0054 and a nitrogen coupling of 13.5 G in aqueous solution.

On the other hand, a search of the literature on radicals with nitro groups shows an exact match for both the $a_N$ value and the *g*-factor for $[HO-C(CH_3)_2NO_2]^{\bullet-}$.[43] This radical was initially discovered through a totally different reaction, namely, the spin-trapping of $^{\bullet}OH$ by $(CH_3)_2C{=}NO_2^-$, the *aci* anion of $(CH_3)_2CHNO_2$:

$$(CH_3)_2C{=}NO_2^- + {}^{\bullet}OH \rightarrow [HO-C(CH_3)_2NO_2]^{\bullet-} \quad (11)$$

The ESR experiment in that reported work was a steady-state, in situ irradiation with no actual spectrum illustrated. For the current work, we repeated this experiment on the spin-trapping of $^{\bullet}OH$ by $(CH_3)_2C{=}NO_2^-$, but in the time-resolved mode. The resulting spectrum contained the same lines as those displayed in Figure 2. The correspondence of the spectrum in Figure 2 with the nitro radical anion produced by a totally different chemical route provides confirmation of the assignment of the ESR spectrum in Figure 2 as that of $[HO-C(CH_3)_2NO_2]^{\bullet-}$. We propose that this radical is formed by reaction 12,

$$(CH_3)_2C^{\bullet}-OH + NO_2^- \rightarrow [HO-C(CH_3)_2NO_2]^{\bullet-} \quad (12)$$

possibly in parallel with the electron transfer (see reaction 10). The broadness of the lines is likely to be caused by unresolved hyperfine splitting by the protons of the two methyl groups. The DFT calculations described previously confirm this interpretation. The computed *g*-factor for the nitro radical anion is 2.0056, the isotropic coupling at nitrogen is calculated to be 25.9 G, both of which are close to the experimental observation, and the averaged splitting due to the methyl protons is −0.3 G. Similar calculations for $(CH_3)_2C^{\bullet}-OH$ yield a *g*-factor of 2.0031 and a large coupling of 19.3 G to six equivalent methyl protons.

Reaction 12 can be confirmed by examining the kinetics of the formation of the adduct and the corresponding decay of $(CH_3)_2C^{\bullet}-OH$ as in Figure 1. A simple analysis of the decay and growth using single exponentials reveals that the 1/*e* period for the decay was 12.5 $\mu$s and that for the 1/*e* buildup time for the growth was 9.0 $\mu$s. This difference in apparent rate constants is quite real and persisted at all concentrations of nitrite and variations in the concentrations of radical scavengers (acetone and 2-propanol). This difference was also apparent in simulations that included the self-reaction of $(CH_3)_2C^{\bullet}-OH$. A higher rate constant was consistently observed for the growth of $[HO-C-(CH_3)_2NO_2]^{\bullet-}$ than for the decay of $(CH_3)_2C^{\bullet}-OH$. Considerable effort was expended in trying various additions to the basic mechanism. These changes did not address this difference in rate constants without introducing other incompatible features, such as a subsequent decay in the ESR of the adduct. The apparent rate constant for the reaction of $(CH_3)_2C^{\bullet}-OH$ with nitrite was in the range of $\sim 1.5 \times 10^6-3 \times 10^6$ $M^{-1}$ $s^{-1}$. Experiments with nitrite concentrations from 5 mM to 25 mM qualitatively showed the expected variation in the observed growth and decay pseudo-first order rate constants. The amplitude of the ESR of the adduct was relatively small, such that only a fraction of the reaction must produce the adduct.

**Alternative Precursors.** Before applying a more quantitative analysis to the ESR observations, it is important to eliminate other possible precursors as sources of $[HO-C(CH_3)_2NO_2]^{\bullet-}$. One consideration is the competition of nitrite for the primary radicals, $^{\bullet}OH$ and $e_{aq}^-$, that will produce $^{\bullet}NO_2$ and $^{\bullet}NO_2^{2-}$, respectively. To access these alternative adduct-formation mechanisms, two experiments were performed with a large excess of nitrite. In one experiment, 0.2 M of nitrite was used with up to 20 mM of acetone at pH 7 (buffered) with 0.1 M of *tert*-butyl alcohol that was added to scavenge hydroxyl radicals ($N_2$-saturated aqueous solutions). Because of the difference in concentrations of nitrite and acetone, the hydrated electrons are scavenged by nitrite (presumably forming $^{\bullet}NO_2^{2-}$ or $H-{}^{\bullet}NO_2^-$). As acetone was added, no adduct ESR spectrum could be detected, which ruled out $^{\bullet}NO_2^{2-}$ or $H-{}^{\bullet}NO_2^-$ as precursor radicals to the adduct radical anions. An analogous experiment was performed to check on the potential involvement of $^{\bullet}NO_2$ as the precursor radical. In these experiments, small amounts of 2-propanol were added to $N_2O$-saturated solutions of 0.2 M nitrite. Again, there was no evidence of the nitro radical anion, and $^{\bullet}NO_2$ was ruled out as the precursor radical.

**Secondary Radical−Radical Reactions.** Note that one alternative to electron transfer (reaction 10) is the addition of nitrite at the oxygen, followed by, or in concert with, a loss of $^{\bullet}NO$ (reactions 13 and 14):

$$(CH_3)_2C^{\bullet}-OH + NO_2^- \rightarrow [HO-C(CH_3)_2ONO]^{\bullet-} \quad (13)$$

$$[HO-C(CH_3)_2ONO]^{\bullet-} + H^+ \rightarrow HO-C(CH_3)_2OH + {}^{\bullet}NO \quad (14)$$

(Also see the theoretical considerations below.) This scheme is equivalent to the electron transfer, because the diol product in reaction 14 is just the acetone hydrate. Nitric oxide is a free radical and should react readily with $(CH_3)_2C^{\bullet}-OH$, as has been suggested.[11] Data exist on the rate constants for the reaction of some radicals with $^{\bullet}NO$:

$$(CH_3)_2C^{\bullet}-OH + {}^{\bullet}NO \rightarrow (CH_3)_2C(OH)NO \quad (15)$$

The rate constant for radicals derived from ethanol (mainly $CH_3-{}^{\bullet}CHOH$) is reported to be $3 \times 10^9$ $M^{-1}$ $s^{-1}$.[44] We have chosen to use this value for reaction 15 in the quantitative treatment of the ESR results, but we have reduced it to $2.4 \times 10^9$ $M^{-1}$ $s^{-1}$, because of the lower temperature. The formation of $^{\bullet}NO$ via reactions 7 and 14, *and* its reaction with $(CH_3)_2C^{\bullet}-OH$, are important additions to the basic adduct-formation mechanism previously presented. A similar reaction involves $^{\bullet}NO_2$ formed from $^{\bullet}OH$ via reaction 5 in competition with reaction 2.

$$(CH_3)_2C^{\bullet}-OH + {}^{\bullet}NO_2 \rightarrow HO-C(CH_3)_2NO_2 \quad (16)$$

All the reactions up to this point do not provide simulations that describe the observations satisfactorily. A reviewer suggested the missing reaction, reaction 17:

$$[HO-C(CH_3)_2NO_2]^{\bullet-} + {}^{\bullet}NO \rightarrow \text{nonradical product} \quad (17)$$

When this reaction is included, the simulation works well.

**Radical Yields.** The modeling of the ESR time profiles included reactions 1−10 and reactions 12−17, plus the self-reaction of $(CH_3)_2C^{\bullet}-OH$, as well as the appropriate Bloch equations. We have not found any value for the rate constant for $k_{16}$ and, therefore, have used the same value as $k_{15}$. (The importance of reaction 16 is greatly reduced in experiments using 0.4 M 2-propanol.) It was assumed that reactions 7 and 14 were rapid. The competition between nitrite and acetone or 2-propanol for the primary radicals was taken into account as

an initial condition. In the case of $H-{}^{\bullet}NO_2^-$, reaction 9 was assumed to be fast. A branching ratio was introduced as the fraction of the total reaction of $(CH_3)_2C^{\bullet}-OH$ with nitrite via addition (reaction 12). The relevant ESR parameters, such as the spin relaxation times, field inhomogeneity parameter, and microwave magnetic field (see the Supporting Information) were as given in Table 1. The relative radiolysis dose was monitored by the electron beam current collected from the ESR cell, and corrections were made for any variations in that quantity (no more than approximately ±5%). The corresponding radical concentration was determined from fitting the decay of the ESR signal of $(CH_3)_2C^{\bullet}-OH$ in an experiment with no added nitrite. Typical initial radical concentrations were ~40 $\mu$M, corresponding ($G = 6$) to a radiation dose of ~65 Gy. A comparison with the ESR signal of ${}^{\bullet}SO_3^-$ was also made, to demonstrate the quantitative accuracy of the method. The only parameter left is the scale factor, which represents an overall measure of the intensity of the line as outlined in the Experimental Section and Supporting Information.

As a demonstration of the method, the yield of $(CH_3)_2C^{\bullet}-OH$ in solutions with 2-propanol and $N_2O$ was compared with that of ${}^{\bullet}SO_3^-$ in a sulfite solution with $N_2O$. To avoid possible problems with congestion of lines in the center of the $(CH_3)_2C^{\bullet}-OH$ spectrum, the kinetic traces were taken of "intensity line 6", at high and low field. These lines are split into two by the −OH proton by ~0.42 G (0.35 G measured at the temperature used). Each of these two lines are further split (with an intensity ratio of 1:5) by the predicted second-order splitting of $12 \times a_H^2(CH_3)/(4\nu_0) \approx 0.6$ G,[34] where $\nu_0 = 3350$ G, using the approximate centerline. The highest-field line ($\Delta B_0 = 35.59$ G) of these four components of "intensity line 6" can be isolated, and its kinetic trace was used in the yield measurements. The average of this kinetic trace with the kinetic trace of the matching low-field line ($\Delta B_0 = -44.22$ G) was taken, to remove the chemically induced dynamic electron polarization (CIDEP). The resulting scale factor was 0.37; that of ${}^{\bullet}SO_3^-$ was 10.7. The yield of $(CH_3)_2C^{\bullet}-OH$ is 100% × (0.37/10.7) × 64/($^5/_6$ × $^6/_2$), which is 89% of that of ${}^{\bullet}SO_3^-$. In this expression, the factor of 64 comes from the total intensity of the 1:6:15:20:15:6:1 pattern associated with the six equivalent protons from the two methyl groups. The factor of $^6/_2$ comes from "intensity line 6" being split into two by the proton of the OH group, and the factor of $^5/_6$ comes from the intensity distribution in the second-order splitting pattern.[34] For measurements in solutions that contain nitrite, a particular second-order component that is part of the central line group and has degeneracy of $^9/_{128}$ was measured. The scale factor in a particular experiment without nitrite was 0.74, and so the total intensity was 10.5. This value is 87% that of 12.1 for ${}^{\bullet}SO_3^-$ on that day and is in agreement with that using the average of the outer lines described previously. Experience with this technique suggests that the accuracy of this determination is approximately ±10%.

A large number of individual experiments were conducted following the decay of this same (central) ESR line, as well as the growth of the central line of the adduct, $[HO-C(CH_3)_2NO_2]^{\bullet-}$. Many different concentrations of acetone and 2-propanol were used, and the nitrite concentration was varied from 0 mM to 25 mM. Many of the experiments used 0.1 M for both acetone and 2-propanol. Because of significant competition for the primary radicals, detailed results of the curve fitting (as in Figure 1) will be presented for two experiments in which the acetone and 2-propanol concentrations were 0.4 and 0.1 M, respectively, in the first case and 0.1 and 0.4 M, respectively, in the second case. A summary of the parameters of the fitting is given in Table 2.

**TABLE 2: Results of Fitting the Electron Spin Resonance (ESR) Time Profiles[a]**

| [nitrite] (mM) | branching ratio[b] | $k_{17}$ ($\times 10^{-8}$ $M^{-1}$ $s^{-1}$) | scale factor for $(CH_3)_2C^{\bullet}-OH$ | scale factor for adduct |
|---|---|---|---|---|
| | [Acetone] = 0.4 M; [2-Propanol] = 0.1 M | | | |
| 5 | 0.33 | 3.0 | 0.81 | 4.1[c] |
| 10 | 0.35 | 3.0 | 0.81 | 4.1[c] |
| 15 | 0.39 | 3.0 | 0.81 | 4.1[c] |
| 20 | 0.39 | 3.0 | 0.80 | 4.1[c] |
| 25 | 0.38 | 3.0 | 0.80 | 4.1[c] |
| | [Acetone] = 0.1 M; [2-Propanol] = 0.4 M | | | |
| 5 | 0.33 | 3.5 | 0.79 | 3.3 |
| 10 | 0.37 | 3.5 | 0.80 | 4.1 |
| 15 | 0.37 | 3.5 | 0.78 | 4.1 |
| 20 | 0.41 | 3.5 | 0.82 | 4.5 |
| 25 | 0.38 | 3.5 | 0.82 | 4.1 |

[a] The value of $k_{10} + k_{12} + k_{13}$ was fixed at $1.6 \times 10^6$ $M^{-1}$ $s^{-1}$, based on fitting the decay of $(CH_3)_2C^{\bullet}-OH$, and represents the total rate for reaction of $(CH_3)_2C^{\bullet}-OH$ with nitrite. [b] $k_{12}/(k_{10} + k_{12} + k_{13})$. [c] Value fixed based on the value for ${}^{\bullet}SO_3^-$ on the same day.

The decay of $(CH_3)_2C^{\bullet}-OH$ was analyzed first, because it is mainly affected by $k_{10} + k_{12} + k_{13}$, which represents the total rate constant for the reaction of $(CH_3)_2C^{\bullet}-OH$ with nitrite. The initial decay is steeper than otherwise predicted, and the inclusion of reaction 16 with ${}^{\bullet}NO_2$ improves the fit. This part of the analysis goes well as for both solutions, and the fitting can be done with a constant value of $k_{10} + k_{12} + k_{13} = 1.6 \times 10^6$ $M^{-1}$ $s^{-1}$. There is considerable reduction in the initial concentration of $(CH_3)_2C^{\bullet}-OH$ at higher nitrite concentration, because of competition for the primary radicals. The almost-constant scale factor for $(CH_3)_2C^{\bullet}-OH$ (for both solutions) shows that the calculations properly account for that fact.

The ESR line studied for $[HO-C(CH_3)_2NO_2]^{\bullet-}$ is quite isolated; therefore, its scaling factor was set at one-third of that for ${}^{\bullet}SO_3^-$, under the same instrumental conditions (12.2 for the first set and 13.0 for the second). Under these constraints, three parameters affect the amplitude of the ESR of $[HO-C(CH_3)_2NO_2]^{\bullet-}$: the rate constant for the reaction of $(CH_3)_2C^{\bullet}-OH$ with nitrite, the branching factor, and the rate constant for reaction 17.

Introduction of reaction 17 affects the amplitude of the ESR of the adduct. At smaller rate constants, it causes the calculated curve to level off at a lower value, such that the apparent 1/e lifetime is shortened. This effect reduces the value of $k_{10} + k_{12} + k_{13}$ that is needed and, indeed, the best value matches that for the $(CH_3)_2C^{\bullet}-OH$ decay. If the value of $k_{17}$ is too high, the curve reaches a maximum and then decreases. This rate constant was adjusted to give a fit to the data. No reason was observed to change the rate constant value for the total reaction of $(CH_3)_2C^{\bullet}-OH$ with nitrite. Results for the other experiments with varying 2-propanol and acetone concentrations were comparable but were not analyzed in the same detail. The approximate constancy of the values for the rate constants and the scaling factors with nitrite concentration shows that the kinetic analysis accounts for the observed behavior quite well.

To summarize, the fraction of $[HO-C(CH_3)_2NO_2]^{\bullet-}$ formed is 0.38 ± 0.04 of the total $(CH_3)_2C^{\bullet}-OH$ reaction with nitrite. In our model, the remaining reaction is electron transfer, reactions 10 or 13 and 14, via an adduct at oxygen. An important reaction for modeling of the kinetics is that of ${}^{\bullet}NO$ with $[HO-C(CH_3)_2NO_2]^{\bullet-}$ (reaction 17).

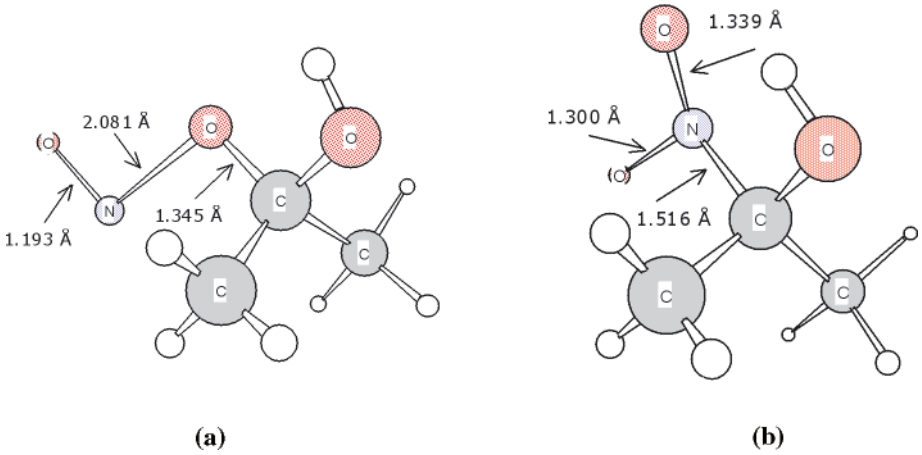


**Figure 3.** Structures from density functional theory (DFT) computations.

**TABLE 3: Relative Free Energies[a] for $NO_2^-$ Addition to 1-Hydroxy-1-methylethyl**

| | Relative Free Energy[a] (kcal/mol) | |
|---|---|---|
| bonding | TS | adduct |
| C−N | 6.0 (17) | −6.1 (−2) |
| C−O | 14 (21) | −18 (−12) |

[a] B3LYP/6-31+G* free energies, relative to separated reactants, including thermal and standard state corrections for 298 K, 1 atm in gas phase and 1 M in solution. Solution values (CPCM HF/6-31+G*//B3LYP/6-31+G*) are given in parentheses.

**Theoretical Considerations of Adduct Formation at Nitrite Oxygens.** The formation reactions of the two adducts ($[HO-C(CH_3)_2NO_2]^{\bullet-}$ and $[HO-C(CH_3)_2-ONO]^{\bullet-}$) were investigated using DFT. The gas-phase optimized structures are shown in Figure 3, and the free energies of the transition states and adducts, relative to the isolated reactants $(CH_3)_2C^{\bullet}-OH$ and $NO_2^-$, are listed in Table 3. Figure 3a shows that the O−N bond in the $[HO-C(CH_3)_2-ONO]^{\bullet-}$ adduct is long (2.081 Å) and, similar to the homologous $HONO^{\bullet-}$ complex,[45] would break apart to form •NO in solution. The products $HO-C(CH_3)_2-O^-$ plus •NO are 22 kcal/mol more stable than $(CH_3)_2C^{\bullet}-OH$ and $NO_2^-$, according to DFT with a single-point solvent calculation. The transition state's free energy for this reaction path is ∼4 kcal/mol higher than the C−N adduct transition state's free energy. However, this difference is not significant, given that the default United Atom Hartree−Fock (UAHF) cavity definition used by the Gaussian98 CPCM solvation model gives solvation energies for anions that may deviate, on average, from the experiment by 4−5 kcal/mol.[46,47] Furthermore, the UAHF cavity definition scheme[48] was not parametrized for transition-state structures. Therefore, C−O adduct formation, in addition to competing parallel reactions (reactions 7 and 8, and/or reactions 11 and 12), could explain the yield of the observed adduct, $[HO-C(CH_3)_2NO_2]^{\bullet-}$, being less than the maximum expected. The absence of additional ESR lines can still be understood, as the radical product •NO is difficult to detect in solution, because it is a $\pi$ radical with orbital angular momentum and broad lines.

The $[HO-C(CH_3)_2NO_2]^{\bullet-}$ structure shown in Figure 3b is more stable, relative to the reactants in gas phase; however, the inclusion of solvation effects leads to it being only slightly more stable than the reactants ($\Delta G_r^\circ = -2$ kcal/mol) in solution (see Table 3). Although this result might suggest reversible formation of the adduct, a TRESR study of reaction 11 precludes this possibility.[49] We conclude that the solution model used in these calculations is simply not accurate enough to predict this equilibrium constant.

## Conclusions

Two observations show that the reaction of $(CH_3)_2C^{\bullet}-OH$ with $NO_2^-$ proceeds via competing pathways, such as reactions 10, 12, and 13; the yield of $[HO-C(CH_3)_2NO_2]^{\bullet-}$ in the electron spin resonance (ESR) experiments is only 38% ± 4% of the reaction of $(CH_3)_2C^{\bullet}-OH$ and nitrite. Furthermore, the absence of observed radical products, other than $[HO-C(CH_3)_2NO_2]^{\bullet-}$, is consistent with the density functional theory (DFT) calculations, which indicates that $[HO-C(CH_3)_2-ONO]^{\bullet-}$ (if formed) readily disassociates to form •NO, which is a radical that is difficult to detect in solution with ESR.

**Acknowledgment.** P.F. and D.M.C. gratefully acknowledge support by the U.S. Department of Energy (DOE) Office of Biological and Environmental Research Environmental Management Science Program. The Pacific Northwest National Laboratory is operated for the DOE by Battelle Memorial Institute. The Notre Dame Radiation Laboratory is supported by the Basic Energy Sciences Division of the DOE; this is Document No. NDRL-4491 from the Notre Dame Radiation Laboratory. The authors thank Professor D. Meisel for critical comments. Professor Kenneth Ruud (University of Tromsoe, Norway) is thanked for a program. The help of a referee is acknowledged for suggesting the reaction of •NO with the nitro radical adduct to explain the faster apparent growth of the adduct compared to the observed decay of the alcohol radicals.

**Supporting Information Available:** Determination of parameters for modeling the time dependence of the ESR signal and coordinates for the structures of transition states leading to C−N and C−O adduct radicals. (PDF format.) This material is available free of charge via the Internet at http://pubs.acs.org.

## References and Notes

(1) Mezyk, S. P.; Bartels, D. M. *J. Phys. Chem. A* **1997**, *101*, 6233−6237.

(2) Lymar, S. V.; Schwarz, H. A.; Czapski, G. *J. Phys. Chem. A* **2002**, *106*, 7245−7250.

(3) Meisel, D.; Camaioni, D.; Orlando, T. Radiation and chemistry in nuclear waste: The $NO_x$ system and organic aging. *ACS Symp. Ser.* **2001**, *778*, 342−361.

(4) Stock, L. M. *The Chemistry of Flammable Gas Generation*; RPP-6664, Rev. 1; CH2M HILL Hanford Group, Inc.: Richland, WA, 2001.

(5) Zeldes, H.; Livingston, R. *J. Am. Chem. Soc.* **1968**, *90*, 4540−4544.

(6) Treinin, A.; Hayon, E. *J. Am. Chem. Soc.* **1970**, *92*, 5821−5828.

(7) Grätzel, M.; Taniguchi, S.; Henglein, A. *Ber. Bunsen−Ges. Phys. Chem.* **1970**, *74*, 488.
(8) Bilski, P.; Chignell, C. F.; Szychlinski, J.; Borkowski, A.; Oleksy, E.; Reszka, K. *J. Am. Chem. Soc.* **1992**, *114*, 549−556.
(9) Pace, M. D. *J. Phys. Chem.* **1994**, *98*, 6251−6257.
(10) Feuer, H. *Tetrahedron Suppl.* **1964**, *20*, 103−117.
(11) Elliot, A. J.; Simons, A. S. *Can. J. Chem.* **1984**, *62*, 1831−1834.
(12) Gilbert, B. C.; Laue, H. A. H.; Norman, R. O. C.; Sealy, R. C. *J. Chem. Soc., Perkin Trans. 2* **1976**, 1040−1044.
(13) Verma, N. C.; Fessenden, R. W. *J. Chem. Phys.* **1976**, *65*, 2139−2155.
(14) Fessenden, R. W.; Hornak, J. P.; Venkataraman, B. *J. Chem. Phys.* **1981**, *74*, 3694−3704.
(15) Madden, K. P.; McManus, H. J. D.; Fessenden, R. W. *Rev. Sci. Instrum.* **1994**, *65*, 49−57.
(16) Duncanson, I. B. *Fusion* **1993**, *XL*, 26.
(17) Wisniowski, P.; Carmichael, I.; Fessenden, R. W.; Hug, G. L. *J. Phys. Chem. A* **2002**, *106*, 4573−4580.
(18) Hug, G. L.; Fessenden, R. W. *J. Phys. Chem. A* **2000**, *104*, 7021−7029.
(19) Frisch, M. J.; Trucks, G. W.; Schlegel, H. B.; Scuseria, G. E.; Robb, M. A.; Cheeseman, J. A.; Zakrzewski, V. G.; Montgomery, J. A.; Jr.; Stratmann, R. E.; Burant, J. C.; Dapprich, S.; Millam, J. M.; Daniels, A. D.; Kudin, K. N.; Strain, M. C.; Farkas, O.; Tomasi, J.; Barone, V.; Cossi, M.; Cammi, R.; Mennucci, B.; Pomelli, C.; Adamo, C.; Clifford, S.; Ochterski, J.; Petersson, G. A.; Ayala, P. Y.; Cui, Q.; Morokuma, K.; Salvador, P.; Dannenberg, J. J.; Malick, D. K.; Rabuck, A. D.; Raghavachari, K.; Foresman, J. B.; Cioslowski, J.; Ortiz, J. V.; Baboul, A. G.; Stefanov; Liu, G.; Liashenko, A.; Piskorz, P.; Komaromi, I.; Gomperts, R.; Martin, R. L.; Fox, D. J.; Keith, T.; Al-Laham, M. A.; Peng, C. Y.; Nanayakkara, A.; Gonzalez, C.; Challacombe, M.; Gill, P. M. W.; Johnson, B.; Chen, W.; Wong, M. W.; Andres, J. L.; Head-Gordon, M.; Replogle, E. S.; Pople, J. A. *Gaussian 98*; Gaussian, Inc.: Pittsburgh, PA, 2001.
(20) Helgaker, T.; Jensen, H. J. A.; Jørgensen, P.; Olsen, J.; Ruud, K.; Ågren, H.; Andersen, T.; Bak, K. L.; Bakken, V.; O.; Christiansen, O.; Dahle, P.; Dalskov, E. K.; Enevoldsen, T.; Fernandez, B.; Heiberg, H.; Hettema, H.; Jonsson, D.; Kirpekar, S.; Kobayashi, R.; Koch, H.; Mikkelsen, K. V.; Norman, P.; Packer, M. J.; Saue, T.; Taylor, P. R.; Vahtras, O. *Dalton, an ab initio electronic structure program*, Release 1.0, 1997.
(21) Becke, A. D. *J. Chem. Phys.* **1993**, *98*, 5648−5652.
(22) Slater, J. C. *The Self-Consistent Field for Molecules and Solids*; McGraw−Hill: New York, 1974.
(23) Becke, A. D. *ACS Symp. Ser.* **1989**, *394*, 165−179.
(24) Vosko, S. H.; Wilk, L.; Nusair, M. *Can. J. Phys.* **1980**, *58*, 1200−1211.
(25) Lee, C.; Yang, W.; Parr, R. G. *Phys. Rev. B* **1988**, *37*, 785−789.
(26) Carmichael, I. *J. Phys. Chem.* **1993**, *97*, 1789−1792.
(27) Neese, F. *J. Chem. Phys.* **2001**, *115*, 11080−11096.
(28) Foresman, J. B.; Keith, T. A.; Wiberg, K. B.; Snoonian, J.; Frisch, M. J. *J. Phys. Chem.* **1996**, *100*, 16098−16104.
(29) Klamt, A.; Schüürmann, G. *J. Chem. Soc. Perkin Trans. 2* **1993**, 799−805.
(30) Barone, V.; Cossi, M. *J. Phys. Chem. A* **1998**, *102*, 1995−2001.
(31) Buxton, G. V.; Greenstock, C. L.; Helman, W. P.; Ross, A. B. *J. Phys. Chem. Ref. Data* **1988**, *17*, 513−886.
(32) Bartels, D. M.; Mezyk, S. P. *J. Phys. Chem.* **1993**, *97*, 4101−4105.
(33) Logager, T.; Sehested, K. *J. Phys. Chem.* **1993**, *97*, 6664−6669.
(34) Fessenden, R. W. *J. Chem. Phys.* **1962**, *37*, 747−750.
(35) Schwarz, H. A.; Dodson, R. W. *J. Phys. Chem.* **1989**, *93*, 409−414.
(36) Lunsford, J. H. *J. Chem. Phys.* **1967**, *46*, 4347−4351.
(37) Lunsford, J. H. *J. Phys. Chem.* **1968**, *72*, 2141−2144.
(38) Fuller, A. M.; Tarr, C. E. *J. Chem. Phys.* **1972**, *56*, 438−440.
(39) Bojko, I.; Lech, J.; Slezak, A. *Acta Phys. Pol. A* **1974**, *45*, 381−386.
(40) Reuveni, A.; Poupko, R.; Luz, Z. *J. Magn. Reson.* **1975**, *18*, 358−366.
(41) Dugas, J.; Bejjaji, B.; Sayah, D.; Trombe, J. C. *J. Solid State Chem.* **1978**, *24*, 143.
(42) Willis, J. S. *J. Chem. Phys.* **1981**, *74*, 979−981.
(43) Eiben, K.; Fessenden, R. W. *J. Phys. Chem.* **1968**, *72*, 3387−3393.
(44) Czapski, G.; Holcman, J.; Bielski, B. H. J. *J. Am. Chem. Soc.* **1994**, *116*, 11465−11469. This rate constant is equivalent to $2.4 \times 10^9$ $M^{-1}$ $s^{-1}$ at 13 °C if the activation energy for the self-reaction of $(CH_3)_2C^{\bullet}-OH$ (14.8 kJ/mol, Ichino, T.; PhD dissertation, University of Notre Dame, 2001) is assumed.
(45) Hug, G. L.; Camaioni, D. M.; Carmichael, I. *J. Phys. Chem. A* **2004**, *108*, 6599−6604.
(46) Takano, Y.; Houk, K. N. *J. Chem. Theory Comput.* **2005**, *1*, 70−77.
(47) Kelly, C. P.; Cramer, C. J.; Truhlar, D. G. *J. Chem. Theory Comput.* **2005**, *1*, 1133−1152.
(48) Barone, V.; Cossi, M.; Tomasi, J. *J. Chem. Phys.* **1997**, *107*, 3210.
(49) Madden, K. P.; Taniguchi, H.; Fessenden, R. W. *J. Am. Chem. Soc.* **1988**, *110*, 2753−2758.